J. Fluid Mech. (2002), *vol.* 463, *pp.* 403–412.
DOI: 10.1017/S0022112002008984 Printed in the United Kingdom

Possible alternative to R_λ-scaling of small-scale turbulence statistics

By REGINALD J. HILL

National Oceanic and Atmospheric Administration, Environmental Technology Laboratory, Boulder, CO 80305-3328, USA

(Received 14 December 2001 and in revised form 10 April 2002)

Traditionally, trends of universal turbulence statistics are presented versus R_λ, which is the Reynolds number based on Taylor's scale λ and the root-mean-square (rms) of a component of velocity u_{rms}. λ and u_{rms}, and hence R_λ, do not have the attribute of universality. The ratio of rms fluid-particle acceleration to the rms of the acceleration caused by the viscous force, $R_{\boldsymbol{a}}$, is an alternative to R_λ. $R_{\boldsymbol{a}}$ is a Reynolds number. It is composed of statistics of the small scales of turbulence. It can be evaluated with single-wire hot-wire anemometry. Like R_λ, it can be partially evaluated by means of flow similarity. Direct measurement of $R_{\boldsymbol{a}}$ is challenging; therefore, $R_{\boldsymbol{a}}$ is not a replacement for R_λ. For isotropic turbulence the relationship between $R_{\boldsymbol{a}}$ and R_λ is given. Anisotropic turbulence is discussed.

1. Introduction

Reynolds (1883) sought, from the Navier–Stokes equation, '... the dependence of the character of motion on a relation between the dimensional properties and the external circumstances of motion'. Assuming that the motion depends on a single velocity scale U and length scale c, Reynolds found that the accelerations are of two distinct types and thereby deduced that the relevant solution of the Navier–Stokes equation 'would show the birth of eddies to depend on some definite value of $c\rho U/\mu$,' where ρ is the mass density of the fluid and μ is the coefficient of viscosity. Reynolds directed exhaustive experiments that demonstrated his deduction, as well as experiments on the stabilization of fluctuating flow. He discovered the sudden onset of flow instability. The Navier–Stokes equation is $\boldsymbol{a} = \partial \boldsymbol{u}/\partial t + \boldsymbol{u} \cdot \nabla \boldsymbol{u} = -\nabla p + \nu \nabla^2 \boldsymbol{u}$, where p is pressure divided by ρ, $\nu = \mu/\rho$ is kinematic viscosity, $\boldsymbol{u}$ is the velocity vector, and $\boldsymbol{a}$ is the acceleration. Batchelor (1967) discussed (in his §4.7) the interpretation of the Reynolds number as a measure of $\boldsymbol{a}$ relative to the viscous term $\nu\nabla^2\boldsymbol{u}$. He noted that the balance of the Navier–Stokes equation can also be parameterized in terms of the relative magnitudes of ∇p and $\nu\nabla^2\boldsymbol{u}$. The latter parameterization does not technically lead to a Reynolds number, but it will be shown that the two parameterizations become equivalent at large Reynolds numbers. Consider the two ratios:

$$R_{\boldsymbol{a}} \equiv \langle \boldsymbol{a} \cdot \boldsymbol{a} \rangle^{1/2} / \langle \nu^2 (\nabla^2 \boldsymbol{u}) \cdot (\nabla^2 \boldsymbol{u}) \rangle^{1/2} \quad (1.1a)$$

$$R_{\nabla p} \equiv \langle \nabla p \cdot \nabla p \rangle^{1/2} / \langle \nu^2 (\nabla^2 \boldsymbol{u}) \cdot (\nabla^2 \boldsymbol{u}) \rangle^{1/2}, \quad (1.1b)$$

where angle brackets denote an average. $R_{\boldsymbol{a}}$ is a Reynolds number in Batchelor's concept, and $R_{\nabla p}$ is a parameterization of the relative magnitudes of ∇p and $\nu\nabla^2\boldsymbol{u}$.

To paraphrase Nelkin's (1994) description of Reynolds number scaling: if two turbulent flows have the same geometry and the same Reynolds number, then their statistics, when appropriately scaled, should be equal. A statistic of the small scales of turbulence is an average of quantities that contain only products of differences, such as two-point velocity difference or derivatives of velocity. Universality of the small scales of turbulence is the hypothesis that every statistic of the small scales, when appropriately scaled, should become independent of the type of flow as Reynolds number increases (Nelkin 1994; Sreenivasan & Antonia 1997); that is, the flow geometry becomes negligible in the limit that the Reynolds number is infinite. Discovering the appropriate scaling that results in universality is the topic of a vast amount of research (Nelkin 1994; Sreenivasan & Antonia 1997) and will not be pursued here. The relevance of universality to real turbulent flows is discussed by Nelkin (1994) and Sreenivasan & Antonia (1997).

The Reynolds number based on the root-mean-square (rms) of the longitudinal-velocity component $u_{rms} \equiv \langle u_1^2 \rangle^{1/2}$ and Taylor's length scale λ is $R_\lambda \equiv u_{rms}\lambda/\nu$, where ν is kinematic viscosity, and $\lambda \equiv u_{rms}/\langle(\partial u_1/\partial x_1)^2\rangle^{1/2}$. Here, u_1 and x_1 are the components of velocity and spatial coordinate in the direction of the 1-axis. For decades, R_λ has been used as the abscissa for presenting statistics that are believed to be universal aspects of small-scale turbulence (such as velocity-derivative statistics normalized by powers of $\langle(\partial u_1/\partial x_1)^2\rangle$). The observed trends as R_λ increases are an often-sought quantification of scaling universality. R_λ has the advantage of being easily measured because it requires only measurement of u_1 (which yields $\partial u_1/\partial x_1$ by means of Taylor's hypothesis); that measurement can be obtained with a single hot-wire anemometer. Alternatively, flow similarity can be used to estimate the energy dissipation rate ε, and by substituting the local-isotropy relationship that $\varepsilon = 15\nu\langle(\partial u_1/\partial x_1)^2\rangle$, R_λ can be obtained from $R_\lambda = u_{rms}^2/(\varepsilon\nu/15)^{1/2}$. Because R_λ depends on u_{rms}, it depends on large-scale geometry of the flow. Nelkin (1994) discussed the non-universal attributes of R_λ. As a result of the non-universality of R_λ, statistics of the small scales, e.g. normalized derivative moments, when graphed with R_λ on the abscissa, can have different curves corresponding to dissimilar flows.

2. Alternative

In addition to graphing such statistics with R_λ on the abscissa, it would seem advantageous to use a quantity on the abscissa that is solely a property of the small scales of turbulence. That advantage has long been recognized (Wyngaard & Tennekes 1970; Van Atta & Antonia 1980; Antonia Chambers & Satyaprakash 1981). Here, we consider the alternative $R_{\boldsymbol{a}}$ defined in (1.1*a*), and determine how it can be measured with an instrument no more complex than a single-wire hot-wire anemometer. Because the intended application is to statistical characteristics of the small scales it is appropriate to simplify $R_{\boldsymbol{a}}$ and $R_{\nabla p}$ on the basis of local isotropy. Indeed, local isotropy is a precondition for universality (Nelkin 1994; Sreenivasan & Antonia 1997). On this basis, $\langle \boldsymbol{a} \cdot \boldsymbol{a} \rangle = \langle \nabla p \cdot \nabla p \rangle + \langle \nu^2 (\nabla^2 \boldsymbol{u}) \cdot (\nabla^2 \boldsymbol{u}) \rangle$ (Obukhov & Yaglom 1951; Hill & Thoroddsen 1997); in which case

$$R_{\boldsymbol{a}} = \sqrt{1 + R_{\nabla p}^2}. \tag{2.1}$$

For high Reynolds numbers $\langle \nabla p \cdot \nabla p \rangle \gg \langle \nu^2 (\nabla^2 \boldsymbol{u}) \cdot (\nabla^2 \boldsymbol{u}) \rangle$ (Hill & Thoroddsen 1997), such that (2.1) becomes $R_{\boldsymbol{a}} \simeq R_{\nabla p}$.

3. Choices for evaluating the variance of $\nu\nabla_{\boldsymbol{x}}^2\boldsymbol{u}$

The spatial correlation of $\nu\nabla_{\boldsymbol{x}}^2\boldsymbol{u}$ is (Obukhov & Yaglom 1951)

$$V_{ij}(\boldsymbol{r}) \equiv \langle \nu^2 \nabla_{\boldsymbol{x}}^2 u_i \nabla_{\boldsymbol{x}'}^2 u_i' \rangle = -\frac{\nu^2}{2}\nabla_{\boldsymbol{r}}^2\nabla_{\boldsymbol{r}}^2 D_{ij}(\boldsymbol{r}), \tag{3.1}$$

where a prime denotes evaluation at a point $\boldsymbol{x}'$; $\boldsymbol{x}$ and $\boldsymbol{x}'$ are independent variables; $\boldsymbol{r} \equiv \boldsymbol{x} - \boldsymbol{x}'$; $\nabla_{\boldsymbol{r}}^2$ is the Laplacian operator in $\boldsymbol{r}$-space; the right-most expression in (3.1) is obtained on the basis of local homogeneity. Let ε denote the energy dissipation rate, and $D_{ij}(\boldsymbol{r})$ and $D_{ijk}(\boldsymbol{r})$ denote the second- and third-order velocity structure functions. The Navier–Stokes equation and local isotropy give (Hill 1997) $\partial_t D_{ij}(\boldsymbol{r}) + \partial_{r_k} D_{ijk}(\boldsymbol{r}) + (4/3)\varepsilon = 2\nu\nabla_{\boldsymbol{r}}^2 D_{ij}(\boldsymbol{r})$; applying the operator $-(\nu/4)\nabla_{\boldsymbol{r}}^2$ to that equation and comparison with (3.1) gives

$$V_{ij}(\boldsymbol{r}) = -(\nu/4)\nabla_{\boldsymbol{r}}^2[\partial_t D_{ij}(\boldsymbol{r}) + \partial_{r_k} D_{ijk}(\boldsymbol{r})]. \tag{3.2}$$

Derivative operators are abbreviated; e.g., $\partial_t = \partial/\partial t$, $\partial_r^2 = \partial^2/\partial r^2$, etc. Summation is implied by repeated indexes. Performing the contraction of (3.1) and (3.2) such that the terms become functions of r and $\nabla_{\boldsymbol{r}}^2 \to \partial_r^2 + (2/r)\partial_r$, we have, on the basis of local isotropy,

$$\begin{aligned} V_{ii}(r) &= -\nu^2\left(\partial_r^4 + \frac{5}{r}\partial_r^3\right)D_{\beta\beta}(r) = -\frac{\nu^2}{2}\left(r\partial_r^5 + 11\partial_r^4 + \frac{24}{r}\partial_r^3\right)D_{11}(r) \\ &= -\partial_t\frac{\nu}{4}[\partial_r^2 + \frac{2}{r}\partial_r]D_{ii}(r) \\ &\quad + \frac{\nu}{2}\left[-\frac{1}{r^3}D_{111}(r) + \left(-\partial_r^3 - \frac{7}{r}\partial_r^2 - \frac{3}{r^2}\partial_r + \frac{6}{r^3}\right)D_{1\beta\beta}(r)\right], \end{aligned}$$

where the 1-axis is parallel to $\boldsymbol{r}$ and subscript β denotes either of the two Cartesian axes perpendicular to the 1-axis. Power-series expansion of the structure functions, followed by differentiation and taking the limit $r \to 0$, gives various formulas for the variance of $\nu\nabla_{\boldsymbol{x}}^2\boldsymbol{u}$:

$$\begin{aligned} V_{ii}(0) &= \langle \nu^2(\nabla^2\boldsymbol{u})\cdot(\nabla^2\boldsymbol{u})\rangle = 12\nu^2\langle(\partial_{x_1}^2 u_\beta)^2\rangle = 35\nu^2\langle(\partial_{x_1}^2 u_1)^2\rangle \\ &= -\tfrac{1}{2}\partial_t\varepsilon - \tfrac{105}{4}\nu\langle(\partial_{x_1}u_\beta)^2\partial_{x_1}u_1\rangle = -\tfrac{1}{2}\partial_t\varepsilon - \tfrac{35}{2}\nu\langle(\partial_{x_1}u_1)^3\rangle, \end{aligned} \tag{3.3}$$

where $\partial_{x_1}^2 \equiv \partial^2/\partial x_1^2$. The term $-(1/2)\partial_t\varepsilon$, which vanishes for local stationarity, is included above, but was neglected by Hill & Thoroddsen (1997); $-(1/2)\partial_t\varepsilon$ is henceforth neglected. The enstrophy generation rate can be written as (Tsinober, Kit & Dracos 1992): $(-35/2)\langle(\partial_{x_1}u_1)^3\rangle = \langle\omega_i\omega_j s_{ij}\rangle = (-4/3)\langle s_{ij}s_{jk}s_{ki}\rangle$; comparing this with the right-most expression in (3.3) gives expressions that can be evaluated by DNS or multi-wire anemometers (Tsinober *et al.* 1992):

$$\langle \nu^2(\nabla^2\boldsymbol{u})\cdot(\nabla^2\boldsymbol{u})\rangle = \nu\langle\omega_i\omega_j s_{ij}\rangle = -\tfrac{4}{3}\nu\langle s_{ij}s_{jk}s_{ki}\rangle, \tag{3.4}$$

where ω_i is vorticity vector and s_{ij} is rate-of-strain tensor.

3.1. *Empirical estimates of* $\langle \nu^2(\nabla^2\boldsymbol{u})\cdot(\nabla^2\boldsymbol{u})\rangle$

Figure 5 of Sreenivasan & Antonia (1997) shows much of the existing data for the velocity-derivative skewness:

$$S \equiv \langle(\partial_{x_1}u_1)^3\rangle/\langle(\partial_{x_1}u_1)^2\rangle^{3/2}.$$

In terms of the skewness, (3.3) gives

$$\langle \nu^2(\nabla^2 \boldsymbol{u}) \cdot (\nabla^2 \boldsymbol{u}) \rangle = 0.30\varepsilon^{3/2}\nu^{-1/2}|S|. \tag{3.5}$$

For $R_\lambda > 400$ Antonia *et al.* (1981) show $|S|$ increasing from 0.5 as $|S| \simeq 0.5(R_\lambda/400)^{0.11}$; (3.5) then gives

$$\langle \nu^2(\nabla^2 \boldsymbol{u}) \cdot (\nabla^2 \boldsymbol{u}) \rangle \simeq 0.078\varepsilon^{3/2}\nu^{-1/2}R_\lambda^{0.11} \quad \text{for} \quad R_\lambda > 400. \tag{3.6}$$

Herring & Kerr (1982) and Kerr (1985) show $|S|$ increasing from 0.074 at $R_\lambda = 0.46$ to become constant at 0.5 for $R_\lambda > 20$. Thus, in the range $20 < R_\lambda < 400$, (3.5) gives

$$\langle \nu^2(\nabla^2 \boldsymbol{u}) \cdot (\nabla^2 \boldsymbol{u}) \rangle \simeq 0.15\varepsilon^{3/2}\nu^{-1/2} \quad \text{for} \quad 20 < R_\lambda < 400. \tag{3.7}$$

The DNS data of Herring & Kerr (1982) suggest that $|S| \simeq R_\lambda/5$ for $R_\lambda < 1$, then $\langle \nu^2(\nabla^2 \boldsymbol{u}) \cdot (\nabla^2 \boldsymbol{u}) \rangle \simeq 0.06\varepsilon^{3/2}\nu^{-1/2}R_\lambda$. If ε and u_{rms} are known from measurements or from flow similarity, then $R_\lambda = u_{rms}^2/(\varepsilon\nu/15)^{1/2}$, which can be used to determine which of the above formulas should be used.

4. Choices for evaluating the variance of ∇p

Poisson's equation, local homogeneity and local isotropy, but no other approximations, result in (Hill & Wilczak 1995)

$$\langle \nabla p \cdot \nabla p \rangle = 4 \int_0^\infty r^{-3}[D_{1111}(r) + D_{\alpha\alpha\alpha\alpha}(r) - 6D_{11\beta\beta}(r)]\, \mathrm{d}r, \tag{4.1}$$

where $D_{1111}(r)$, $D_{\alpha\alpha\alpha\alpha}(r)$ and $D_{11\beta\beta}(r)$ are components of the fourth-order velocity structure-function tensor, defined by $D_{ijkl}(\boldsymbol{r}) \equiv \langle (u_i - u_i')(u_j - u_j')(u_k - u_k')(u_l - u_l') \rangle$; the 1-axis is parallel to the separation vector $\boldsymbol{r}$; α and β denote the Cartesian axes perpendicular to the 1-axis. Thus, α and β are 2 or 3; equally valid options under local isotropy are $\alpha = \beta$ or $\alpha \neq \beta$.

As noted by Hill & Wilczak (1995), Hill & Boratav (1997), and Nelkin & Chen (1998), there is enough cancellation between the positive and negative parts of the integrand, i.e. between $r^{-3}[D_{1111}(r)+D_{\alpha\alpha\alpha\alpha}(r)]$ and $-r^{-3}6D_{11\beta\beta}(r)$, to make evaluation of the integral $\int_0^\infty r^{-3}[D_{1111}(r)+D_{\alpha\alpha\alpha\alpha}(r)-6D_{11\beta\beta}(r)]\,\mathrm{d}r$ difficult by means of experimental or DNS data. Hill & Wilczak (1995) argued that the ratio

$$H_\chi \equiv \frac{\displaystyle\int_0^\infty r^{-3}[D_{1111}(r) + D_{\alpha\alpha\alpha\alpha}(r) - 6D_{11\beta\beta}(r)]\,\mathrm{d}r}{\displaystyle\int_0^\infty r^{-3}D_{1111}(r)\,\mathrm{d}r} = \frac{\langle \nabla p \cdot \nabla p \rangle}{4\displaystyle\int_0^\infty r^{-3}D_{1111}(r)\,\mathrm{d}r},$$

is a universal constant at high Reynolds numbers. Universality of H_χ is equivalent to the assertion that $\langle \nabla p \cdot \nabla p \rangle$ scales with $\int_0^\infty r^{-3}D_{1111}(r)\,\mathrm{d}r$ at high Reynolds numbers. Hill & Wilczak (1995) pointed out that the utility of determining H_χ is that the pressure-gradient variance can then be measured with a single-wire hot-wire anemometer by means of

$$\langle \nabla p \cdot \nabla p \rangle = 4H_\chi \int_0^\infty r^{-3}D_{1111}(r)\,\mathrm{d}r. \tag{4.2}$$

Thus, the choices for evaluating $\langle \nabla p \cdot \nabla p \rangle$ are (4.1), or (4.2) (for which the values of H_χ are discussed below), or to use the values of $\langle \nabla p \cdot \nabla p \rangle$ obtained from the DNS data of Vedula & Yeung (1999) and Gotoh & Fukayama (2001) in the range $20 \lesssim R_\lambda \lesssim 400$, or (4.3)–(4.4), also discussed below.

4.1. *Empirical estimates of* $\langle \nabla p \cdot \nabla p \rangle$

Asymptotic expressions for $\langle \nabla p \cdot \nabla p \rangle$ derived from empirical data for the shape of $D_{1111}(r)$ at high Reynolds numbers substituted into (4.2) are (Hill 2002)

$$\langle \nabla p \cdot \nabla p \rangle \simeq 3.1 H_\chi \varepsilon^{3/2} \nu^{-1/2} F^{0.79} \simeq 3.9 H_\chi \varepsilon^{3/2} \nu^{-1/2} R_\lambda^{0.25} \quad \text{for} \quad R_\lambda \gtrsim 400, \tag{4.3}$$

where

$$F \equiv \langle (\partial_{x_1} u_1)^4 \rangle / \langle (\partial_{x_1} u_1)^2 \rangle^2 .$$

The empirical data for (4.3) are for $R_\lambda \gtrsim 400$, but Hill (2002) shows that (4.3) is in quantitative agreement with DNS for $R_\lambda \gtrsim 200$. The right-most expression in (4.3) is obtained from the data for F of Antonia *et al.* (1981), which are in agreement with data at $R_\lambda = 10^4$ of Kolmyansky, Tsinober & Yorish (2001). The low-Reynolds-number asymptote given by Hill (2002) is

$$\langle \nabla p \cdot \nabla p \rangle \simeq 0.11 \varepsilon^{3/2} \nu^{-1/2} R_\lambda \quad \text{for} \quad R_\lambda \lesssim 20. \tag{4.4}$$

Using DNS data, it is preferable to evaluate H_χ from

$$H_\chi = \langle \nabla p \cdot \nabla p \rangle / \left[4 \int_0^\infty r^{-3} D_{1111}(r)\, \mathrm{d}r \right];$$

this avoids the statistical uncertainty caused by the cancellations within the integrand of (4.1). Vedula & Yeung (1999) evaluated H_χ using DNS data with $R_\lambda < 230$; they found that H_χ varied from 0.55 at $R_\lambda = 20$ to a constant value of about 0.65 in the range $80 < R_\lambda < 230$. For $H_\chi = 0.65$, (4.3) agrees quantitatively with the DNS data in table 1 of Gotoh & Fukayama (2001) for $R_\lambda \geqslant 387$, and (4.3) is a good approximation for $R_\lambda \gtrsim 200$ (Hill 2002). Since the asymptotic formula (4.3) is thereby verified with $H_\chi = 0.65$, the range of validity of $H_\chi = 0.65$ seems to extend to the highest R_λ for which Antonia *et al.* (1981) obtained F, namely $R_\lambda \simeq 10^4$, but it might extend to $R_\lambda = \infty$. On that basis, H_χ increases from its the low-Reynolds-number asymptote (Hill 1994) of 0.36 as $R_\lambda \longrightarrow 0$, to 0.55 at $R_\lambda = 20$, and to $H_\chi \simeq 0.65$ in the range $R_\lambda > 80$.

5. Isotropic turbulence

For isotropic turbulence there is a one-to-one relationship between $R_{\boldsymbol{a}}$ and R_λ; it is shown in figure 1 with $R_{\nabla p}$ included. Figure 1 was obtained from (2.1) by use of (3.6)–(3.7), (4.3)–(4.4) and (3.5) and the discussions following those equations. That is: For $R_\lambda \lesssim 1$, $\langle \nu^2 (\nabla^2 \boldsymbol{u}) \cdot (\nabla^2 \boldsymbol{u}) \rangle \simeq 0.06 \varepsilon^{3/2} \nu^{-1/2} R_\lambda$ and (4.4) give $R_{\nabla p} \simeq (12 R_\lambda / 35 |S|)^{1/2} \simeq (12/7)^{1/2} \simeq 1.3$. For $1 \lesssim R_\lambda \lesssim 20$, (3.5) and (4.4) give $R_{\nabla p} \simeq (12 R_\lambda / 35 |S|)^{1/2}$ such that the data of Kerr (1985) for $|S|$ gives the plus symbols in figure 1. For $20 \lesssim R_\lambda \lesssim 400$, (3.5) with $|S| = 0.5$ gives $R_{\nabla p} \simeq 2.6 (\langle \nabla p \cdot \nabla p \rangle / \varepsilon^{3/2} \nu^{-1/2})^{1/2}$ such that data for $\langle \nabla p \cdot \nabla p \rangle$ tabulated by Vedula & Yeung (1999) give the asterisks in figure 1 and data for $\langle \nabla p \cdot \nabla p \rangle$ given by Gotoh & Fukayama (2001) give the triangles in figure 1. For $R_\lambda \gtrsim 400$, (3.6) and (4.3) give $R_{\nabla p} \simeq [(3.1 H_\chi \varepsilon^{3/2} \nu^{-1/2} F^{0.79}) / (0.3 \varepsilon^{3/2} \nu^{-1/2} |S|)]^{1/2} \simeq 5.7 R_\lambda^{0.07}$. Finally, $R_{\boldsymbol{a}}$ is calculated from the above determinations of $R_{\nabla p}$ using (2.1), i.e. $R_{\boldsymbol{a}} = (1 + R_{\nabla p}^2)^{1/2}$. In figure 1, the upper symbols are $R_{\boldsymbol{a}}$ and are not distinguishable from the symbols for $R_{\nabla p}$ where $R_\lambda \geqslant 20$. The solid line depicting $R_{\boldsymbol{a}} \simeq R_{\nabla p} \simeq 5.7 R_\lambda^{0.07}$ is extended to $R_\lambda = 100$ to show, by comparison with the data of Vedula & Yeung and Gotoh & Fukayama, that it is a good approximation for $R_\lambda \gtrsim 200$.

From $R_\lambda = 1$ to 10^4 in figure 1, $R_{\nabla p}$ changes by one decade and $R_{\boldsymbol{a}}$ by less. The magnitude of $R_{\boldsymbol{a}}$ relative to R_λ or of R_λ to any other Reynolds number is not relevant

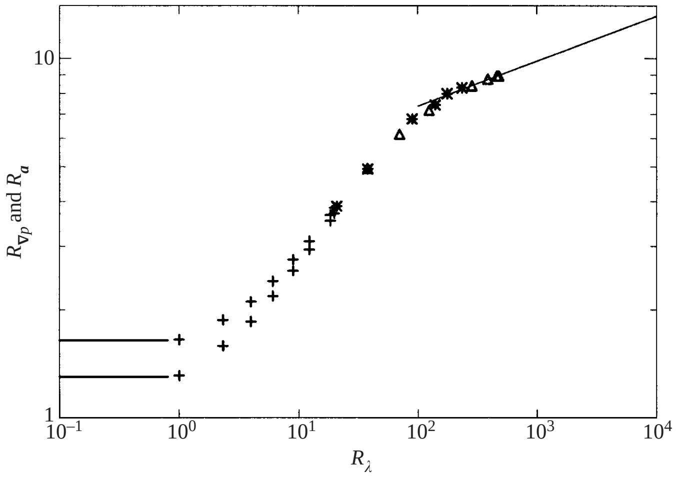

FIGURE 1. Relationship between R_a and R_λ (upper curve) and between $R_{\nabla p}$ and R_λ (lower curve) for isotropic turbulence. The straight lines are from the asymptotic formulas given in the text, and the symbols are from DNS data as described in the text.

to scaling. Figure 1 is based on nearly isotropic data only for $R_\lambda \lesssim 400$; for $R_\lambda \gtrsim 400$ the data used for F in (4.3) and S in (3.5) are those of Antonia *et al.* (1981) which consist, in part, of atmospheric surface layer data at $R_\lambda \gtrsim 2000$; those data are in agreement with data at $R_\lambda = 10^4$ by Kolmyansky *et al.* (2001). The assumption is that for $R_\lambda \gtrsim 400$ the turbulence is sufficiently locally isotropic that the relationships of F and S to R_λ measured by Antonia *et al.* (1981) do not differ significantly from what they would be for isotropic turbulence. Some support for the assumption is that the asymptote $R_{\nabla p} \simeq 5.7 R_\lambda^{0.07}$ in figure 1 agrees with the nearly isotropic data for R_λ as small as 200. However, further confirmation must await DNS and experiments on nearly isotropic turbulence at higher Reynolds numbers than have been attained to date.

5.1. *Relationship to recent data*

The DNS data of Vedula & Yeung (1999), Gotoh & Rogallo (1999) and Gotoh & Fukayama (2001) are in the range of R_λ where $|S| \simeq 0.5$ so (3.7) gives $\langle \nu^2 (\nabla^2 \boldsymbol{u}) \cdot (\nabla^2 \boldsymbol{u}) \rangle \simeq 0.15 \varepsilon^{3/2} \nu^{-1/2}$. In their figure 1, Vedula & Yeung (1999) show a ratio that they call ζ, which equals $R_{\nabla p}^2$, as well as a quantity $a_0^{(I)} \equiv \langle \boldsymbol{a} \cdot \boldsymbol{a} \rangle / (3 \varepsilon^{3/2} \nu^{-1/2}) \simeq 0.05 R_a^2$, where $\langle \nu^2 (\nabla^2 \boldsymbol{u}) \cdot (\nabla^2 \boldsymbol{u}) \rangle \simeq 0.15 \varepsilon^{3/2} \nu^{-1/2}$ was used; they graphed both ζ and $a_0^{(I)}$ versus R_λ. Similarly, Gotoh & Rogallo (1999) and Gotoh & Fukayama (2001) show $F_{\nabla p} = 3 a_0^{(I)} = \langle \boldsymbol{a} \cdot \boldsymbol{a} \rangle / (\varepsilon^{3/2} \nu^{-1/2}) \simeq 0.15 R_a^2$ versus R_λ in their figures 1 and 2. Therefore, the above-mentioned graphs show $R_{\nabla p}^2$ and R_a^2 as R_λ varies. Reversing the role of ordinates and abscissas in their graphs and in figure 1, the graphs show R_λ for nearly isotropic turbulence as the universal Reynolds number R_a varies.

6. Anisotropic turbulence

By the definition of anisotropic turbulence, the value of $\langle u_1^2 \rangle$ depends on the direction of $\boldsymbol{r}$. Thus, R_λ does also. With R_λ on the abscissa, the appearance of graphed statistics can change depending on which velocity component is used to calculate R_λ. For anisotropic and/or inhomogeneous flows the Reynolds number is

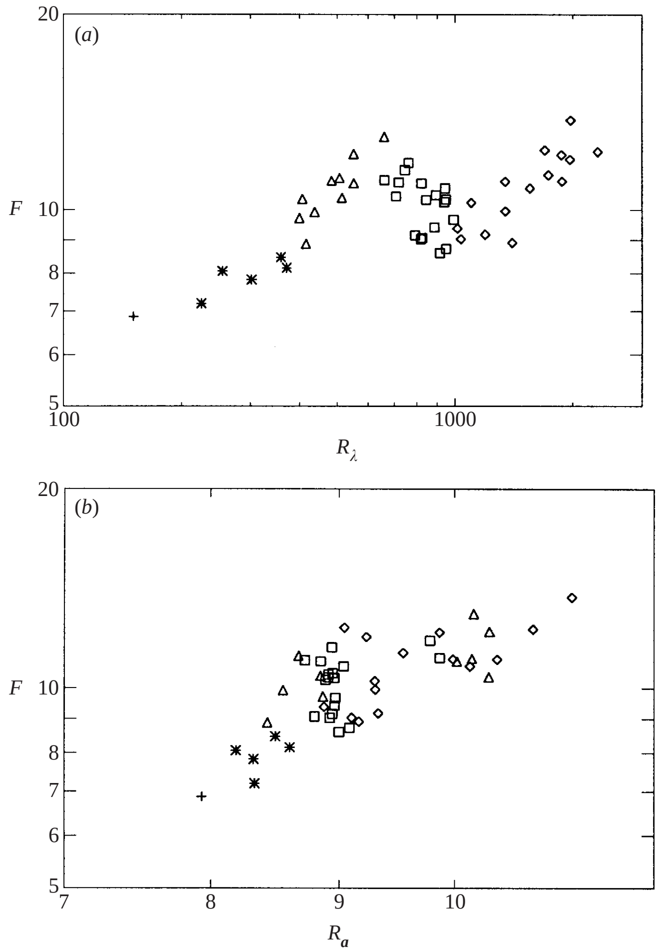

FIGURE 2. (*a*) Velocity derivative flatness data of Belin *et al.* (1997) graphed versus R_λ with different symbols for different ranges of R_λ. (*b*) Same data and symbols as in (*a*), but graphed versus R_a. Scatter of the data is increased relative to (*a*) because of scatter in the data for S used to evaluate R_a (see text).

not the only parameter required to study the statistics of small scales. The most useful dimensionless parameters should be identified for each flow. Consider F at the highest R_λ in figure 6 of Sreenivasan & Antonia (1997). Most of those F values are from the atmospheric surface layer data of Wyngaard & Tennekes (1970) for which the definition of R_λ included the variance of horizontal velocity (denoted by $\langle u^2 \rangle$ in their equation (25)). Consider the portion of their data obtained during daytime convective conditions. For data from the surface layer under convective conditions, the variance of the streamwise component of velocity relative to the friction velocity depends on the ratio of height above ground to both the Monin–Obukhov length and the depth of the entire convective boundary layer. Without axes that represent the dependence on such other relevant parameters, a projection of data onto the F versus R_λ plane produces scatter in the data. A simpler case is uniform shear flow, for which both Reynolds number and mean shear are relevant parameters (see Saddoughi & Veeravalli 1994 and Schumacher, Sreenivasan & Yeung 2002; the former reference discusses dimensionless shear parameters in detail).

Turbulent flow in a cylinder driven by counter-rotating blades has several modes of large-scale structure (Zocchi *et al.* 1994; Voth *et al.* 2002) and is anisotropic at large scales, but local isotropy is approached in the centre of the cylinder (La Porta *et al.* 2001) at high Reynolds numbers. Belin *et al.* (1997) measured S, F, $H_5^* \equiv \langle|\partial_{x_1}u_1|^5\rangle/\langle(\partial_{x_1}u_1)^2\rangle^{5/2}$ and $H_6 \equiv \langle(\partial_{x_1}u_1)^6\rangle/\langle(\partial_{x_1}u_1)^2\rangle^3$ in the flow between counter-rotating blades at positions displaced from the centre toward both the wall and blades (as described in Zocchi *et al.* 1994); they graph F, H_5^* and H_6 with R_λ on the abscissa; each statistic has a maximum and a minimum. Figure 2(a) reproduces their graph of F versus R_λ. Their values of F, H_5^* and H_6 are related to each other by power laws that Belin *et al.* (1997) describe as impressive despite the complexity of the evolution of the same quantities with R_λ. From the choices for evaluation, we select (3.5) and (4.3) and obtain $R_{\nabla p} = (2.0F^{0.79}/0.3|S|)^{1/2}$ and thereby evaluate $R_{\nabla p}$ and $R_{\boldsymbol{a}}$ using the data for S and F of Belin *et al.* The result gives F versus $R_{\boldsymbol{a}}$ in figure 2(b). Unfortunately, their S values are too scattered for such a calculation (the scatter is caused by noise; P. Tabeling, private communication 2001). The maximum and minimum in figure 2(a) appear to be absent in figure 2(b), but the scatter might obscure some other complicated behaviour. As an example, consider that the power law $|S| = 0.25F^{3/8}$ seems to be accurate for a variety of flows for $R_\lambda \gtrsim 400$ (Champagne 1978; Antonia *et al.* 1981). If the noise-free S value in the flow of Belin *et al.* (1997) were related to F by some power law, then $R_{\boldsymbol{a}} \simeq R_{\nabla p} = (2.0F^{0.79}/0.3|S|)^{1/2}$ would be related to F by a power law. From the results of Belin *et al.*, S, F, H_5^* and H_6 would then all be related to $R_{\boldsymbol{a}}$ by power laws, despite the complexity of the evolution of those quantities with R_λ. Perhaps this possibility will motivate efforts to achieve accurate measurement of S and of the more basic measures of $\langle \nu^2(\nabla^2\boldsymbol{u})\cdot(\nabla^2\boldsymbol{u})\rangle$ in (3.3)–(3.4).

7. Summary and comment

As defined in (1.1a), $R_{\boldsymbol{a}}$ is a Reynolds number; it is the ratio of rms fluid-particle acceleration to the rms of acceleration caused by the viscous force; it is composed of statistics of the small scales of turbulence; it can be used as a universal abscissa for judging the universality of turbulence statistics. Although $R_{\nabla p}$ is not strictly a Reynolds number, it also can be used as a universal abscissa. At high Reynolds numbers, $R_{\nabla p} \simeq R_{\boldsymbol{a}}$. $R_{\nabla p}$ can be evaluated with single-wire hot-wire anemometry and by flow similarity; use of (2.1) then determines $R_{\boldsymbol{a}}$. For DNS studies, $R_{\boldsymbol{a}}$ can be calculated from its definition (1.1a). Experimental determination of $R_{\boldsymbol{a}}$ is difficult; thus $R_{\boldsymbol{a}}$ is an alternative to R_λ, not a replacement for it.

Improved data for $\langle \nu^2(\nabla^2\boldsymbol{u})\cdot(\nabla^2\boldsymbol{u})\rangle$ and $\langle \nabla p\cdot\nabla p\rangle$, and their relationships to the local-isotropy formulas (3.1)–(3.4) and (4.1)–(4.2), as well as improved data for H_χ would be useful in the present context. For evaluation of the correlation of viscous force, it is clear from figure 13 of Vedula & Yeung (1999) that DNS must have especially fine spatial resolution. Use of the single-wire anemometer approximations in (3.3) suggest that further studies of the accuracy of local isotropy are needed. To calculate $R_{\boldsymbol{a}}$ by means of the local isotropy formulas, the flow should approximately attain local isotropy.

Models of small-scale statistics of turbulence should be expressed in terms of universal attributes instead of in terms of R_λ. For example, in table II of Belin *et al.* (1997), the model by Pullin & Saffman (1993) is in good agreement with data when it is judged in terms of power laws between derivative moments, but in relatively poor agreement when judged in terms of power laws between normalized derivative moments and R_λ. R_λ can be specific to the flow geometry.

The author thanks P. Tabeling for sending the data of Belin *et al.*, and thanks the organizers of the Hydrodynamics Turbulence Program held at the Institute for Theoretical Physics, UCSB, whereby this research was supported in part by the National Science Foundation under grant number PHY94-07194.

REFERENCES

Antonia, R. A., Chambers, A. J. & Satyaprakash, B. R. 1981 Reynolds number dependence of high-order moments of the streamwise turbulent velocity derivative. *Boundary-Layer Met.* **21**, 159–171.

Batchelor, G. K. 1967 *An Introduction to Fluid Dynamics*. Cambridge University Press.

Belin, F., Maurer, J., Tabeling, P. & Willaime, H. 1997 Velocity gradient distributions in fully developed turbulence: An experimental study. *Phys. Fluids* **9**, 3843–3850.

Champagne, F. H. 1978 The fine-scale structure of the turbulent velocity field. *J. Fluid Mech.* **86**, 67–108.

Gotoh, T. & Fukayama, D. 2001 Pressure spectrum in homogeneous turbulence. *Phys. Rev. Lett.* **86**, 3775–3778.

Gotoh, T. & Rogallo, R. S. 1999 Intermittency and scaling of pressure at small scales in forced isotropic turbulence. *J. Fluid Mech.* **396**, 257–285.

Herring, J. R. & Kerr, R. M. 1982 Comparison of direct numerical simulations with predictions of two-point closures for isotropic turbulence convecting a passive scalar. *J. Fluid Mech.* **118**, 205–219.

Hill, R. J. 1994 The assumption of joint Gaussian velocities as applied to the pressure structure function. *NOAA Tech. Rep.* ERL 451–ETL-277 (www.bldrdoc.gov/library).

Hill, R. J. 1997 Applicability of Kolmogorov's and Monin's equations of turbulence. *J. Fluid Mech.* **353**, 67–81.

Hill, R. J. 2002 Scaling of acceleration in locally isotropic turbulence. *J. Fluid Mech.* **452**, 361–370.

Hill, R. J. & Boratav, O. N. 1997 Pressure statistics for locally isotropic turbulence. *Phys. Rev.* E **56**, R2363–R2366.

Hill, R. J. & Thoroddsen, S. T. 1997 Experimental evaluation of acceleration correlations for locally isotropic turbulence. *Phys. Rev.* E **55**, 1600–1606.

Hill, R. J. & Wilczak, J. M. 1995 Pressure structure functions and spectra for locally isotropic turbulence. *J. Fluid Mech.* **296**, 247–269.

Kerr, R. M. 1985 Higher-order derivative correlations and the alignment of small-scale structures in isotropic numerical turbulence. *J. Fluid Mech.* **153**, 31–58.

Kolmyansky, M., Tsinober, A. & Yorish, S. 2001 Velocity derivatives in the atmospheric surface layer at $Re_\lambda = 10^4$. *Phys. Fluids* **13**, 311–314.

La Porta, A., Voth, G. A., Crawford, A. M., Alexander, A. & Bodenschatz, E. 2001 Fluid particle accelerations in fully developed turbulence. *Nature* **409**, 1017–1019.

Nelkin, M. 1994 Universality and scaling in fully developed turbulence. *Adv. Phys.* **43**, 143–181.

Nelkin, M. & Chen, S. 1998 The scaling of pressure in isotropic turbulence. *Phys. Fluids* **10**, 2119–2121.

Obukhov, A. M. & Yaglom, A. M. 1951 The microstructure of turbulent flow. *Prikl. Mat. Mekh.* **15**, 3–26.

Pullin, D. I. & Saffman, P. G. 1993 On the Lundgren-Townsend model of turbulent fine scales. *Phys. Fluids* A **5**, 126–145.

Reynolds, O. 1883 An experimental investigation of the circumstances which determine whether the motion of water shall be direct or sinuous, and of the law of resistance in parallel channels. *Phil. Trans. R. Soc. Lond.* **174**, 935–986.

Saddoughi, S. G. & Veeravalli, S. V. 1994 Local isotropy in turbulent boundary layers at high Reynolds number. *J. Fluid Mech.* **268**, 333–372.

Schumacher, J., Sreenivasan, K. R. & Yeung, P. K. 2002 Derivative moments in turbulent shear flows. *Phys. Rev.* E (submitted).

Sreenivasan, K. R. & Antonia, R. A. 1997 The phenomenology of small scale turbulence. *Annu. Rev. Fluid Mech.* **29**, 435–472.

Taylor, G. I. 1935 Statistical theory of turbulence. *Proc. R. Soc. Lond.* **151**, 465–478.

Tsinober, A., Kit, E. & Dracos, T. 1992 Experimental investigation of the field of velocity gradients in turbulent flows. *J. Fluid Mech.* **242**, 169–192.

Van Atta, C. W. & Antonia, R. A. 1980 Reynolds number dependence of skewness and flatness factors of turbulent velocity derivatives. *Phys. Fluids* **23**, 252–257.

Vedula, P. & Yeung, P. K. 1999 Similarity scaling of acceleration and pressure statistics in numerical simulations of isotropic turbulence. *Phys. Fluids* **11**, 1208–1220.

Voth, G. A., La Porta, A., Crawford, A. M., Alexander, J. & Bodenschatz, E. 2002 Measurement of particle accelerations in fully developed turbulence. *J. Fluid Mech.* (to appear); xxx.lanl.gov/physics/0110027.

Wyngaard, J. C. & Tennekes, H. 1970 Measurements of the small-scale structure of turbulence at moderate Reynolds numbers. *Phys. Fluids* **13**, 1962–1969.

Zocchi, G., Tabeling, P., Maurer, J. & Willaime, H. 1994 Measurement of the scaling of the dissipation at high Reynolds numbers. *Phys. Rev.* E **50**, 3693–3700.